

Highlights

Hebbian Semi-Supervised Learning in a Sample Efficiency Setting

Gabriele Lagani, Fabrizio Falchi, Claudio Gennaro, Giuseppe Amato

- We propose a semi-supervised learning approach that combines Hebbian learning with Stochastic Gradient Decent (SGD) on object recognition tasks with Deep Convolutional Neural Networks (DCNNs).
- Unlabeled training samples are used for a Hebbian pre-training phase, where nonlinear Hebbian Principal Component Analysis (HPCA) learning rule is used to train internal layers (both convolutional and fully connected);
- Then, labeled training samples and SGD are used to train a classifier, obtained as a final fully connected layer, on the features extracted from previous layers;
- The results are compared from a sample efficiency perspective with those obtained by a baseline network trained, end-to-end with backprop, on the labeled samples;
- Different datasets and different regimes of sample efficiency are explored, and it is shown that the proposed semi-supervised approach (Hebbian + SGD) outperforms full backprop in almost all the cases where a limited number of labeled samples is available.

Hebbian Semi-Supervised Learning in a Sample Efficiency Setting

Gabriele Lagani^{a,*}, Fabrizio Falchi^b, Claudio Gennaro^b, Giuseppe Amato^b

^aComputer Science Department, University of Pisa, Pisa, Italy

^bISTI - CNR, Pisa, Italy

Abstract

We propose to address the issue of sample efficiency, in Deep Convolutional Neural Networks (DCNN), with a semi-supervised training strategy that combines Hebbian learning with gradient descent: all internal layers (both convolutional and fully connected) are pre-trained using an unsupervised approach based on Hebbian learning, and the last fully connected layer (the classification layer) is trained using Stochastic Gradient Descent (SGD). In fact, as Hebbian learning is an unsupervised learning method, its potential lies in the possibility of training the internal layers of a DCNN without labeled examples. Only the final fully connected layer has to be trained with labeled examples.

We performed experiments on various object recognition datasets, in different regimes of sample efficiency, comparing our semi-supervised (Hebbian for internal layers + SGD for the final fully connected layer) approach with end-to-end supervised backpropagation training. The results show that, in regimes where the number of available labeled samples is low, our semi-supervised approach outperforms full backpropagation in almost all the cases.

Keywords: Convolutional Neural Networks, Computer Vision, Semi-Supervised Learning, Hebbian Learning, Sample Efficiency.

PACS: 0000, 1111

2000 MSC: 0000, 1111

1. Introduction

In recent years, Deep Neural Networks (DNNs) have achieved impressive results in learning tasks such as computer vision [1], reinforcement learning [2], natural language processing [3].

Today's neural networks are generally trained using the error backpropagation algorithm (backprop). Backpropagation reaches high accuracy when a large number of labeled samples are available for training. However, gathering labeled samples is expensive, requires a significant amount of human work, and, in many applications, a large amount of training data is simply not available.

Therefore, researchers started to investigate strategies for sample efficient learning [4, 5, 6, 7, 8, 9, 10]. In this setting, only a small number of labeled samples is assumed to be available. On the other hand, gathering unlabeled samples is relatively simple; therefore, these approaches exploit unlabeled samples to perform unsupervised training in addition to the supervised training

process, leading to the so called *semi-supervised* learning technique. It is well known that unsupervised pre-training helps initializing the network weights in the neighborhood of a good local optimum [4, 5], thus easing convergence in a successive supervised fine-tuning phase. Current semi-supervised approaches leverage autoencoder architectures for the unsupervised part of the task [7, 8, 9], although they are still based on backprop. A more recent approach, SimCLR [10], exploits data augmentation and an unsupervised contrastive criterion.

In this work, we address the sample efficiency issue by proposing a semi-supervised learning approach, where an initial unsupervised learning step, using unlabeled data, is followed by a supervised learning step using a small amount of labeled data. To perform the unsupervised learning step we explore the use of the Hebbian learning paradigm, which mimics more closely the synaptic adaptation mechanisms found in biological brains, according to neuroscientists. Hebbian learning is a local learning rule [11, 12], i.e. it does not require error backpropagation, and it does not require supervision. Moreover, the capabilities of biological

*Corresp. author. E-mail: gabriele.lagani@phd.unipi.it

brains to learn and generalize only from a limited number of labeled samples make this approach appealing for the sample efficient learning setting. Note also that backprop-based approaches are considered to be biologically implausible [13].

The main contributions of this paper are the following:

- We propose a semi-supervised learning approach that combines Hebbian learning with Stochastic Gradient Descent (SGD) on object recognition tasks with Deep Convolutional Neural Networks (DCNNs).
 - Unlabeled training samples are used for a Hebbian pre-training phase, where nonlinear Hebbian Principal Component Analysis (HPCA) learning rule is used to train internal layers (both convolutional and fully connected);
 - Then, labeled training samples and SGD are used to train a classifier, obtained as a final fully connected layer, on the features extracted from previous layers;
- The results are compared from a sample efficiency perspective with those obtained by a baseline network trained, end-to-end with backprop, on the labeled samples;
- Different datasets and different regimes of sample efficiency are explored, and it is shown that the proposed semi-supervised approach (Hebbian + SGD) outperforms full backprop in almost all the cases where a limited number of labeled samples is available.

The remainder of this paper is structured as follows: Section 2 gives an overview on related work concerning semi-supervised training and Hebbian learning; Section 3 illustrates the sample efficiency problem. Section 4 defines our approach to sample efficiency based on semi-supervised Hebbian + SGD learning; Section 5 provides a background on the Hebbian learning rule that we used in this work; Section 6 delves into the details of our experimental setup; In Section 7, the results of our simulations are illustrated; Finally, Section 8 presents our conclusions and outlines possible future developments.

2. Related work

In this section, we present an overview of related work concerning both semi-supervised training and Hebbian learning.

2.1. Semi-supervised training and sample efficiency

Early work on deep learning had to face problems related to convergence to poor local minima during the training process, which led researchers to exploit a pre-training phase that allowed them to initialize network weights in a region near a good local optimum [4, 5]. In these studies, greedy layerwise pre-training was performed by applying unsupervised autoencoder models layer by layer, thus training each layer to provide a compressed representation of the input for a successive decoding stage. It was shown that such pre-training was indeed helpful to obtain a good initialization for a successive supervised training stage. In successive works, the idea of enhancing neural network training with an unsupervised learning objective was considered [6, 7, 8, 9]. In [7], Variational Auto-Encoders (VAE) are considered to perform an unsupervised pre-training phase using a limited amount of labeled samples. Later on, [8] and [9] also relied on autoencoding architectures to augment supervised training with unsupervised reconstruction objectives, showing that joint optimization of supervised and unsupervised losses helped to regularize the learning process. In [14], joint supervised and unsupervised training was again considered, but the unsupervised learning part was based on manifold learning techniques. More recently, the SimCLR approach [10] was proposed, which uses a Contrastive Loss approach to perform the unsupervised learning part. The approach relies on data augmentation, in order to produce transformed variants of a given input, and the unsupervised loss basically imposes hidden representations to match for transformed variants generated from the same input.

2.2. Hebbian learning

Several variants of Hebbian learning rules were developed over the years, such as Hebbian learning with Winner-Takes-All (WTA) competition [15], Self-Organizing Maps [16], Hebbian learning for Principal Component Analysis (PCA) [11, 17, 18, 19], Hebbian/anti-Hebbian learning [20, 21]. A brief overview is given in section 5. However, it was only recently that Hebbian learning started gaining attention in the context of DNN training [22, 23, 24, 25, 26, 27]. In [25], a Hebbian learning rule based on inhibitory competition was used to train a neural network composed of fully connected layers on object recognition tasks. Instead, the Hebbian/anti-Hebbian learning rule developed in [20] was applied in [24] to extract convolutional features that were shown to be effective for classification. Convolutional layers were also considered in [22, 23], where a Hebbian approach based on

WTA competition was used to train the feature extractors. However, the previous approaches were based on relatively shallow network architectures (2-3 layers). A further step was taken in [26, 27], where a Hebbian WTA learning rule was investigated for training a 6-layer Convolutional Neural Network (CNN). Also, a supervised variant of Hebbian learning was proposed to train the final classification layer. Hybrid network models were also considered, in which some layers were trained using backprop and others using Hebbian learning. The results suggested that Hebbian learning is suitable for training early feature detectors, as well as higher network layers, but not very effective for training intermediate network layers. Furthermore, Hebbian learning was successfully used to retrain the higher layers of a pre-trained network, achieving results comparable to backprop, but requiring fewer training epochs, thus suggesting potential applications in the context of transfer learning (see also [28, 29, 30]).

3. Sample efficiency scenario

Training neural networks with supervision requires gathering a large amount of labeled training samples. This can be quite expensive, since it requires a considerable amount of human intervention for manually labeling collected samples. On the other hand, gathering unlabeled samples is generally considerably cheaper. In real world scenarios, one might need to solve AI problems for which only a small amount of labeled samples is available. In some cases, it is possible to start from a neural network pre-trained on a similar task, for which a good number of labeled samples was available, and just fine-tune it on the target task using the available labeled samples (thus performing transfer learning [31]). However, in many cases, the target task might considerably differ from the original task.

In such cases, it would be desirable to have a training algorithm that is capable of exploiting the latent information contained in large collections of unlabeled samples, while using only a small set of labeled samples for a successive stage of supervised training.

In fact, in applications where gathering large amounts of manually labeled data would be too expensive, it is often possible to collect a considerable amount of unlabeled samples at a relatively cheap cost. Therefore, it is desirable for an algorithm to be able to acquire knowledge about the data using only unlabeled samples and learning to extract possibly useful features by, for example, learning to distinguish frequent shapes and patterns, or detecting rarely occurring anomalies. However, a fully supervised, backprop-based, approach, typ-

ically requires many labeled samples to achieve a good performance.

Formally, the sample efficiency learning scenario can be stated as follows: let \mathcal{T} be our *training set*, let $s \in \mathcal{T}$ be an element (called *training sample*) of the training set. Elements of \mathcal{T} are drawn from a statistical distribution with *probability density function (pdf)* $p(s)$:

$$s \sim p(s) \quad (1)$$

Let $N = |\mathcal{T}|$ be the number of training samples in \mathcal{T} (where $|\cdot|$ denotes the cardinality of the set). Let \mathcal{L} be another set, whose elements $l \in \mathcal{L}$ are called *labels*. Let

$$\phi : \mathcal{T} \rightarrow \mathcal{L} \quad (2)$$

be a function that maps training samples to a corresponding label. This function is unknown, except for a subset of \mathcal{T} for which labels are given. Specifically, we define the *labeled set* as a subset $\mathcal{T}_L \subset \mathcal{T}$ of elements for which the image of the function ϕ is known:

$$\mathcal{T}_L = \{s \in \mathcal{T} \mid \phi(s) \text{ is known}\} \quad (3)$$

Let's define the *unlabeled set* \mathcal{T}_U as the complement of \mathcal{T}_L w.r.t. \mathcal{T} . Therefore, for the unlabeled set, label information is not available; nonetheless, samples from \mathcal{T}_U are drawn from the same statistical distribution as the samples from \mathcal{T}_L and \mathcal{T} , i.e. from $p(s)$. In a *sample efficiency* scenario, the number of samples in \mathcal{T}_L is typically much smaller than the total number of samples N in \mathcal{T} , i.e.

$$|\mathcal{T}_L| \ll |\mathcal{T}| \quad (4)$$

In particular, an *r%-sample efficiency* scenario is characterized by

$$|\mathcal{T}_L| = \frac{r}{100} |\mathcal{T}| \quad (5)$$

i.e. the size of the labeled set is *r%* that of the whole training set (labeled plus unlabeled). A neural network is required to approximate, by a training process, the function ϕ . For a given \mathcal{T} and a given *r%-sample efficiency* regime, we define a neural network to *perform better* than another if it reaches higher accuracy in mapping samples to correct labels (according to function ϕ), given that both networks are trained using \mathcal{T}_L and \mathcal{T}_U splits that are compliant with the considered *r%-sample efficiency* scenario, i.e. both networks have been trained with a number of labeled samples equal to *r%* of the total number of samples in \mathcal{T} . The training process can use both samples from \mathcal{T}_L , with the associated labels (i.e. training *with supervision*), and samples from \mathcal{T}_U (i.e. training *without supervision*).

4. Hebbian-SGD Semi-Supervised learning approach

Traditional supervised approaches based on back-propagation work well provided that the size of the labeled set is sufficiently large, but they do not exploit the unlabeled set. In the semi-supervised approach that we propose, we aim to learn an approximation of function ϕ by means of a two stage process: first, we run an unsupervised training stage in which we use samples from \mathcal{T}_U in order to learn latent representations for samples drawn from $p(s)$; subsequently, we use the small number of available labeled samples from \mathcal{T}_L , with the corresponding labels, in a supervised training phase. During the first phase, latent representations are obtained from hidden layer of a DCNN, which are trained using an unsupervised, biologically plausible, Hebbian learning algorithm. During the second phase, supervised training is applied on a final linear classifier, by running a SGD optimization procedure using only the few labeled samples at our disposal.

Specifically, we propose the following semi-supervised learning approach, which combines Hebbian learning with SGD, applied to a deep convolutional neural network architecture as the one in Figure 1:

1. the internal layers of the neural network are trained without supervision using the Hebbian learning rule, given in Eq. 12 discussed in Section 5, and the unlabeled samples \mathcal{T}_U , independently from the final fully connected layer, used as classifier;
2. the final fully connected layer, used as classifier, is trained with SGD, freezing weight of previous layers, and using only the few labeled examples in \mathcal{T}_L .

As we will shown in the following, we found that our semi-supervised approach achieves interesting results in low sample efficiency regimes. In fact, when only a small number of labeled samples is used (roughly from 1% to 5% of the total number of training samples contained in the considered datasets), our approach generally offers better results than full backprop training. Thus it represents a valid solution to real life applications, where the number of available labeled samples is small.

In the experiments, discussed below, we compared the performance of our approach with the full backprop, considering various levels of sample efficiency, and varying the number of hidden layers of the DCNN. In fact, we run different experiments in which the final classifier is placed on top of a different inner layer of the network, in order to evaluate the quality of the feature

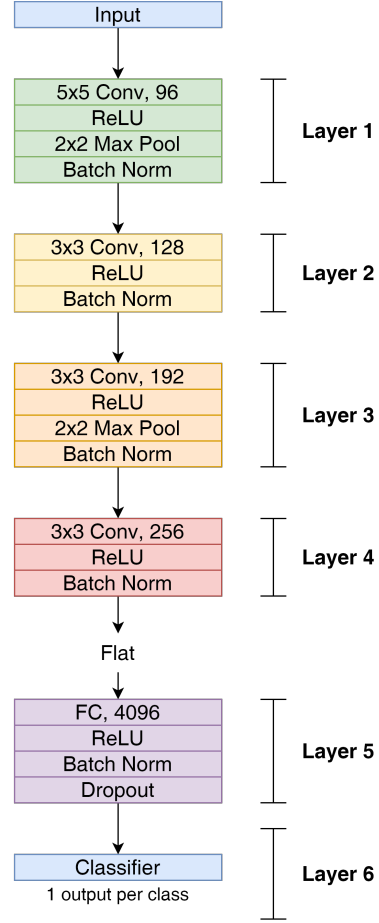


Figure 1: The neural network used for the experiments.

representations extracted at different network depths in the classification task. As we will show later, our approach performs better than simple end-to-end backprop training in almost all the cases when we consider low sample efficiency scenarios, where the percentage of labeled samples is between 1% and 5% (i.e. r %-sample efficiency scenarios with $1 \leq r \leq 5$).

5. Background on Hebbian learning

For a given neuron, the weight updates according to the Hebbian learning rule, in its most basic form, can be expressed as [11]:

$$\mathbf{w}_{new} = \mathbf{w}_{old} + \Delta \mathbf{w} \quad (6)$$

where \mathbf{w}_{new} is the updated weight vector, \mathbf{w}_{old} is the old weight vector, and $\Delta \mathbf{w}$ is the weight update. The latter term is computed as follows:

$$\Delta \mathbf{w} = \eta \mathbf{y} \mathbf{x} \quad (7)$$

Here, \mathbf{x} is the input vector of the neuron, \mathbf{w} is its weight vector, $y = \mathbf{w}^T \mathbf{x}$ is its output, and η is the learning rate. According to this rule, the weight on a given synapse is increased when the input on that synapse and the output of the neuron are simultaneously high, so that correlation between simultaneously active neurons is reinforced.

The learning rule above is unstable, in that neuron weights are allowed to grow unbounded. To prevent this circumstance, a weight decay term is typically added, as suggested, for example, in works on competitive learning [15, 16]:

$$\Delta \mathbf{w} = \eta y \mathbf{x} - \eta y \mathbf{w} = \eta y (\mathbf{x} - \mathbf{w}) \quad (8)$$

The rule above can be easily interpreted intuitively: when an input vector is presented to the neuron, its vector of weights takes a small step towards the input, so that the neuron will exhibit a stronger response if a similar input is presented again in the future. When a series of inputs drawn from a cluster are presented to the neuron, the weight vector converges towards the cluster center (Figure 2).

In a complex neural network, several neurons are involved in representing the input. Ideally, we would like each neuron to learn to represent a different property of the inputs. Therefore, we need a strategy to prevent neurons from learning redundant information. The Winner-Takes-All (WTA) [15] strategy was proposed for this purpose. It was motivated by the observation that biological neural networks exhibit inhibitory competition, i.e. when a neuron fires, it provokes the inhibition of neighboring neurons. In the WTA strategy, when an input is presented to a neural network layer, a *winner* neuron is determined. This is the one whose weight vector is closest to the current current input, and it is the only neuron allowed to perform a weight update according to Eq. 8. In this way, if a similar input is presented again in the future, the same neuron will be more likely to win again. At the same time, different neurons are induced to represent different properties of the inputs, namely the centroids of the clusters formed by the input data points (Fig. 3).

The WTA provides a *quantized* encoding scheme, in which one particular neuron activates to encode a particular input. However, it has been argued that a distributed type of encoding would be more powerful [32, 33], in which different neurons simultaneously activate to encode different properties of the input.

A more distributed coding scheme can be achieved if neuron weight vectors are trained to encode the principal components of the input data. This can be

achieved by Hebbian Principal Component Analysis (HPCA) learning rules, in an efficient, online manner [11, 17, 19, 18]. The Hebbian PCA learning rule is obtained by minimizing the *representation error* loss function, defined as:

$$L(\mathbf{w}_i) = E\left[\left(\mathbf{x} - \sum_{j=1}^i y_j \mathbf{w}_j\right)^2\right] \quad (9)$$

where, in this case, the subscript i is used to denote the i^{th} neuron in the layer and $E[\cdot]$ is the mean value operator. This objective reduces to classical PCA, in the case of linear neurons and zero centered data, which requires to maximize output variance, while the weight vectors are subject to orthonormality constraints, as shown in [11, 17, 19, 18]. In the following, we assume that the input data are centered around zero. If this is not true, we just need to subtract the average $E[\mathbf{x}]$ from the inputs beforehand.

Minimizing the objective in Eq. 9 leads to the following Hebbian PCA learning rule [11, 17, 19, 18]:

$$\Delta \mathbf{w}_i = \eta y_i (\mathbf{x} - \sum_{j=1}^i y_j \mathbf{w}_j) \quad (10)$$

In particular, we consider the case in which neurons have nonlinear activation functions $f(\cdot)$, so that the representation error becomes:

$$L(\mathbf{w}_i) = E\left[\left(\mathbf{x} - \sum_{j=1}^i f(y_j) \mathbf{w}_j\right)^2\right] \quad (11)$$

Minimization of this objective [18, 19] leads to the nonlinear Hebbian PCA learning rule that we used in our experiments:

$$\Delta \mathbf{w}_i = \eta f(y_i) (\mathbf{x} - \sum_{j=1}^i f(y_j) \mathbf{w}_j) \quad (12)$$

6. Experimental setup

In the following, we describe the details of our experiments and comparisons, discussing the network architecture and the training procedure¹.

¹The code to reproduce the experiments described in this paper is available at:

<https://github.com/GabrieleLagani/HebbianPCA/tree/hebbpca>.

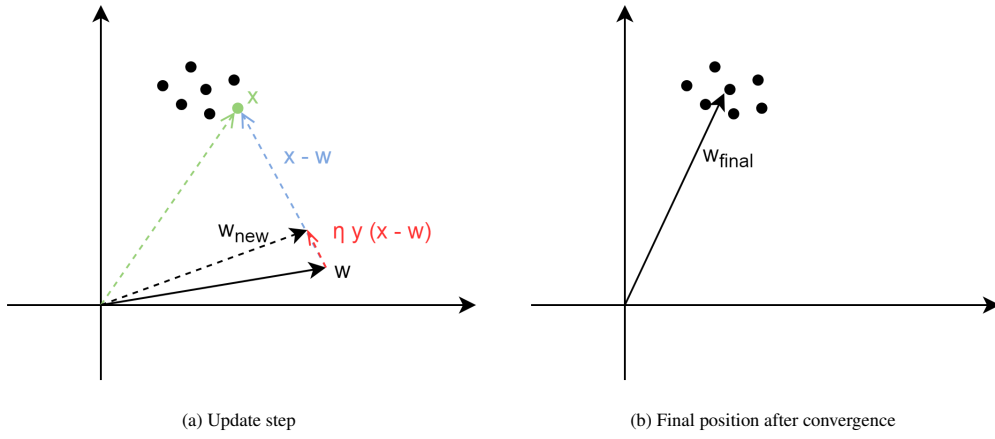


Figure 2: Hebbian updates with weight decay.

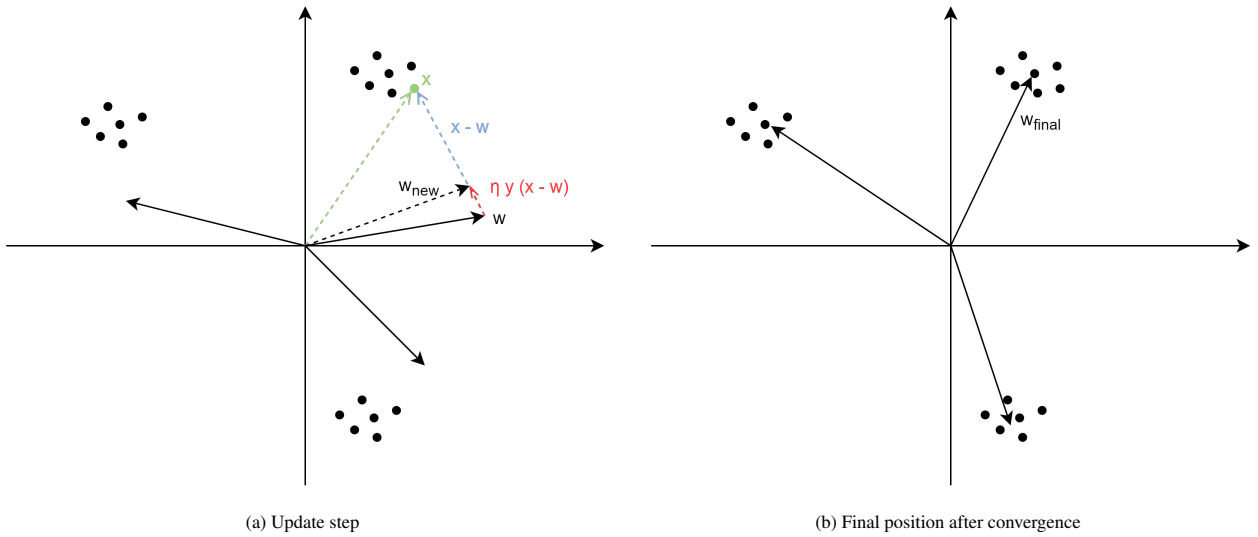


Figure 3: Hebbian updates with Winner-Takes All competition.

6.1. Datasets used for the experiments

The experiments were performed on the following datasets: CIFAR10, CIFAR100 [34] and TinyImageNet [35].

The CIFAR10 dataset contains 50,000 training images and 10,000 test images, belonging to 10 classes. Moreover, the training images were randomly split into a training set of 40,000 images and a validation set of 10,000 images.

The CIFAR100 dataset also contains 50,000 training images and 10,000 test images, belonging to 100 classes. Also in this case, the training images were randomly split into a training set of 40,000 images and a validation set of 10,000 images.

The TinyImageNet dataset contains 100,000 training images and 10,000 test images, belonging to 200 classes. Moreover, the training images were randomly split into a training set of 90,000 images and a validation set of 10,000 images.

We considered a range of sample efficiency regimes, i.e. we assumed that only a limited number of labeled samples was available for training. We considered the following sample-efficiency regimes: the amount of labeled samples were respectively 1%, 2%, 3%, 4%, 5%, 10%, 25% and 100% of the whole training set. This corresponds to 400, 800, 1,200, 1,600, 2,000, 4,000, 10,000, 40,000 labeled samples for the CIFAR10 and CIFAR100 datasets, and to 900, 1,800, 2,700, 3,600, 4,500, 9,000, 22,500 labeled samples for TinyImageNet.

6.2. Network architecture and training

We considered a six layer neural network as shown in Fig. 1: five deep layers plus a final linear classifier, obtained as a fully connected layer on top of previous layer. The various layers were interleaved with other processing stages (such as ReLU nonlinearities, max-pooling, etc.). The architecture was inspired by AlexNet [36], but with slight modifications in order to reduce the overall computational cost of training.

For each sample efficiency regime, we trained a deep network with our semi-supervised approach, using the Hebbian PCA (HPCA) rule in Eq. 12 (in which the nonlinearity was set to the ReLU function) in the internal layers, followed by the SGD training step in the classification layer only.

For each sample efficiency configuration we also created a baseline for comparison, training an identical network using SGD with error backpropagation in all layers, in a supervised fashion.

As already stated, while supervised training can only use the labeled samples, the unsupervised training step

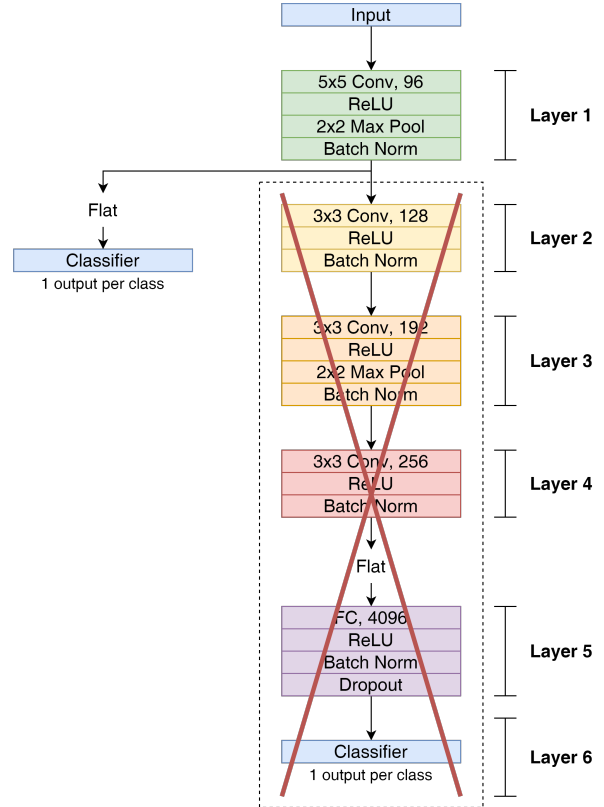


Figure 4: A neural network is cut in correspondence of layer 1, and a linear classifier is placed on top of the features extracted from that layer, in order to evaluate their quality in classification tasks.

(for the internal layers) can leverage both labeled and unlabeled samples.

6.3. Testing sample efficiency at different layer depths

In our experiments, in addition to evaluate the entire network trained as discussed above, we also evaluated the sample efficiency capability on the various internal layers of the trained models. To this end, we cut the networks in correspondence of the output of the various layers and we trained a new linear classifier on top of each already pre-trained layer (for instance, Fig. 4 shows a classifier placed on top of the features extracted from the first layer), and the resulting accuracy was evaluated. These new classifiers were trained with supervision using SGD, hence using only the limited number of training samples given by the sample efficiency regime considered, freezing the pre-trained internal layers. This process was done both for the HPCA trained network, and the SGD trained network, used as baseline, so we were able to compare the performance of the two networks. More details are given below.

6.4. Details of training

We implemented our experiments using PyTorch. Training was performed in 20 epochs using mini-batches of size 64. Networks were fed input images of size 32x32 pixels. Experiments were performed using five different seeds for the Random Number Generator (RNG), averaging the results and computing 95% confidence intervals.

For SGD training of the baseline network, the initial learning rate was set to 10^{-3} and kept constant for the first ten epochs, while it was halved every two epochs for the remaining ten epochs. We also used momentum coefficient 0.9, Nesterov correction, dropout rate 0.5 and L2 weight decay penalty coefficient set to $5 \cdot 10^{-2}$ for CIFAR10, 10^{-2} for CIFAR100 and $5 \cdot 10^{-3}$ for Tiny-ImageNet. Cross-entropy loss was used as optimization metric.

In the HPCA training, the learning rate was set to 10^{-3} . No L2 regularization or dropout was used in this case, since the learning method did not present overfitting issues.

The linear classifiers placed on top of the various network layers were trained with supervision using SGD in the same way as we described above for training the whole network, but the L2 penalty term was reduced to $5 \cdot 10^{-4}$.

To obtain the best possible generalization, *early stopping* was used in each training session, i.e. we chose as final trained model the state of the network at the epoch when the highest validation accuracy was recorded.

All the above mentioned hyperparameters resulted from a parameter search aimed at maximizing the accuracy on the respective datasets.

6.5. Further details on HPCA training

When HPCA training was used, we noticed that BatchNorm (BN) on higher layers was disruptive. The reason is that HPCA uses the variance along input dimensions in order to understand which dimensions in the input space are more relevant. BN, however, normalizes the input distribution, so that each input dimension is rescaled to have unit variance, thus causing a loss of information that would have been useful to HPCA. For this reason, we defined a modified BN version as follows: instead of dividing each input dimension by the respective variance estimated from samples, we divided each input dimension by the average of all the variances estimated for all the input dimensions. This allowed us to rescale input dimensions in order to have a fixed variance, on average, while at the same time maintaining the relative order of each of the input dimensions in terms

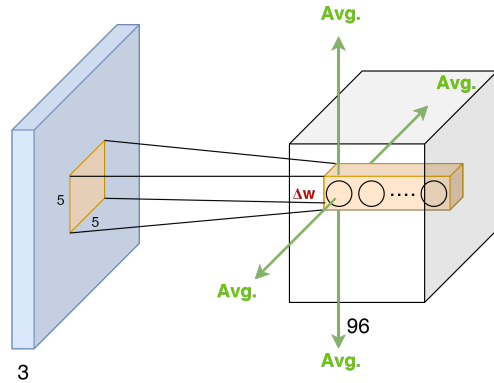


Figure 5: Update averaging over horizontal and vertical dimensions.

of their variances. The modified BN was applied to layers 4 and 5 of the network during HPCA training. On the other hand, standard BN was found to be preferable for earlier layers, where feature detectors had not yet developed a task specificity.

In convolutional layers, the HPCA rule was applied to convolutional filters at each offset. In order to preserve weight sharing, the resulting weight updates were averaged along the height, width and batch dimensions (Fig. 5), and the result was the actual weight update that was applied to the convolutional filter.

7. Results and discussion

In this section, the experimental results obtained with each dataset are presented and analyzed. Results are reported in Tab. 1 Tab. 2, and Tab. 3 for CIFAR10, CIFAR100, and TinyImageNet, respectively. After training the entire network, independently, with backprop (BP) and with Hebbian PCA (HPCA), we placed and trained a linear classifier on top of the various layers. The linear classifier was trained, on top of the two pre-trained networks, using supervised learning with a number of labeled samples corresponding to the various sample efficiency regimes considered. Tables report the classification accuracy, along with the 95% confidence intervals, for the various sample efficiency regimes, when the classification layer is placed on top of the various internal layers (L_1, \dots, L_5).

7.1. CIFAR10

Tab. 1 reports the top-1 accuracy results obtained on the CIFAR10 dataset. We only report top-1 accuracy, given that CIFAR10 contains only 10 classes. At a first glance, we see that in regimes where a limited number of labeled samples is available, the Hebbian approach

Table 1: CIFAR10 accuracy (top-1) and 95% confidence intervals, obtained with a linear classifier on top of various layers, for the various sample efficiency regimes. Results obtained with backprop (BP) and Hebbian PCA (HPCA) training are compared. It is possible to observe that, in regimes where the number of available samples is low (roughly between 1% and 5% of the total available samples), HPCA outperforms backprop in almost all the cases, leading to an improvement up to almost 5% (on layer 3, in the 1% regime).

Regimes	Method	L1	L2	L3	L4	L5
1%	BP	33.27 \pm 0.44	34.56 \pm 0.34	36.80 \pm 0.52	35.47 \pm 0.58	35.18 \pm 0.57
	HPCA	36.78 \pm 0.46	37.26 \pm 0.14	41.31 \pm 0.57	39.33 \pm 0.72	38.46 \pm 0.44
2%	BP	37.33 \pm 0.25	39.01 \pm 0.19	42.34 \pm 0.51	41.50 \pm 0.32	41.10 \pm 0.39
	HPCA	41.13 \pm 0.30	41.63 \pm 0.18	45.76 \pm 0.41	44.70 \pm 0.45	43.15 \pm 0.45
3%	BP	40.49 \pm 0.26	41.90 \pm 0.40	45.13 \pm 0.53	45.26 \pm 0.22	44.52 \pm 0.24
	HPCA	44.16 \pm 0.42	44.84 \pm 0.08	48.92 \pm 0.17	47.70 \pm 0.57	45.60 \pm 0.27
4%	BP	43.38 \pm 0.22	45.43 \pm 0.18	49.51 \pm 0.49	48.96 \pm 0.48	48.80 \pm 0.24
	HPCA	46.37 \pm 0.16	47.16 \pm 0.28	50.70 \pm 0.26	49.45 \pm 0.15	47.75 \pm 0.54
5%	BP	45.11 \pm 0.21	47.57 \pm 0.29	50.61 \pm 0.32	50.54 \pm 0.23	50.42 \pm 0.14
	HPCA	47.51 \pm 0.65	48.69 \pm 0.37	51.69 \pm 0.56	50.44 \pm 0.43	48.51 \pm 0.32
10%	BP	51.60 \pm 0.40	54.60 \pm 0.31	57.97 \pm 0.28	57.63 \pm 0.23	57.30 \pm 0.22
	HPCA	52.57 \pm 0.29	53.29 \pm 0.25	56.09 \pm 0.38	54.24 \pm 0.28	52.68 \pm 0.36
25%	BP	60.43 \pm 0.26	64.96 \pm 0.18	66.63 \pm 0.17	68.04 \pm 0.05	68.04 \pm 0.20
	HPCA	58.30 \pm 0.28	59.20 \pm 0.24	59.98 \pm 0.20	57.54 \pm 0.20	56.46 \pm 0.18
100%	BP	61.59 \pm 0.08	67.67 \pm 0.11	73.87 \pm 0.15	83.88 \pm 0.04	84.71 \pm 0.02
	HPCA	64.69 \pm 0.29	65.92 \pm 0.14	64.43 \pm 0.21	61.24 \pm 0.22	61.16 \pm 0.33

achieves better results than the BP counterpart, in almost all the cases. On the other hand, when the number of available labeled samples becomes larger, BP is able to exploit supervision and improve over HPCA in almost all the cases. Specifically, we see that for efficiency regimes up to 3%, HPCA is better than BP, when tested in all layers of the network. We can observe that HPCA generally outperforms backprop by roughly 1-3 percent points, reaching a peak of almost 5 percent points on layer 3, in the 1% sample efficiency regime. At 4% efficiency regime, we note that HPCA is still performing better than BP for the first 4 layers, while BP performs better than HPCA when the linear classifier is put on top of the fifth layer. This effect continues for higher efficiency regimes, where we see that increasing the amount of labeled samples, reduces the highest layer where HPCA has better performance than BP. So, we observe that for 5% efficiency regimes HPCA is better than BP up to Layer 3. Still, in low sample efficiency regimes (between 1% and 5%), HPCA outperforms backprop in almost all the cases. At 10% efficiency regimes HPCA is better only when the linear classifier is trained on top of Layer 1. BP always outperforms HPCA when 100% labeled examples are used.

To explain this behaviour we can observe that, on one hand, when the amount of labeled samples increases,

BP is able to effectively take advantage of the supervised information and extract more useful knowledge from training data. This starts to be seen from the highest layers of the network, where the supervision signal is stronger. Increasing the amount of labeled training data brings this effect down up to the first network layer. On the other hand, unsupervised Hebbian learning signal, which is driven by the inputs, is stronger in the first layers, where coherence between input and output of neurons is more meaningful, and layers tend to adapt faster to the unsupervised stimuli.

7.2. CIFAR100

Since CIFAR10 contained just 10 different classes, to validate our observations with a similar, yet more difficult scenario, we also performed tests with CIFAR100, containing 100 classes. In Tab. 2 the top-5 accuracy results obtained on the CIFAR100 dataset are shown. These experiments confirm our previous observations. The results show that, in regimes where a limited number of labeled samples is available (between 1% and 5%), our semi supervised approach, based on Hebbian learning, achieves better results than BP in almost all the cases. Except for 1% sample efficiency regime, where the difference in the results is not really significant, for regimes up to 3% HPCA is always better than BP. In

Table 2: CIFAR100 accuracy (top-5) and 95% confidence intervals obtained with a linear classifier on top of various layers, for the various sample efficiency regimes. Results obtained with backprop (BP) and Hebbian PCA (HPCA) training are compared. It is possible to observe that, in regimes where the number of available samples is low (roughly between 1% and 5% of the total available samples), HPCA outperforms backprop in almost all the cases. Even though, in various cases, the improvement is small, it becomes significant in some scenarios, where peaks of improvement up to 2% are observed (on layers 3 and 4).

Regimes	Method	L1	L2	L3	L4	L5
1%	BP	22.56 ± 0.53	22.73 ± 0.28	23.41 ± 0.44	20.85 ± 0.58	21.88 ± 0.30
	HPCA	21.90 ± 0.33	22.23 ± 0.50	22.98 ± 0.18	20.88 ± 0.43	21.90 ± 0.55
2%	BP	28.99 ± 0.49	29.07 ± 0.68	30.75 ± 0.34	27.67 ± 0.37	28.18 ± 0.35
	HPCA	29.08 ± 0.31	29.40 ± 0.23	32.22 ± 0.28	29.20 ± 0.46	28.95 ± 0.35
3%	BP	31.77 ± 0.42	32.56 ± 0.51	34.06 ± 0.41	31.81 ± 0.33	32.45 ± 0.23
	HPCA	32.07 ± 0.46	33.04 ± 0.30	36.41 ± 0.15	33.67 ± 0.39	32.61 ± 0.51
4%	BP	34.74 ± 0.29	35.88 ± 0.30	37.63 ± 0.19	35.92 ± 0.35	36.52 ± 0.37
	HPCA	35.34 ± 0.40	35.97 ± 0.27	39.85 ± 0.35	37.23 ± 0.19	36.05 ± 0.37
5%	BP	36.84 ± 0.23	37.70 ± 0.32	39.70 ± 0.21	38.42 ± 0.32	39.21 ± 0.65
	HPCA	37.28 ± 0.40	37.75 ± 0.24	42.12 ± 0.49	39.37 ± 0.18	37.84 ± 0.22
10%	BP	42.04 ± 0.24	44.98 ± 0.23	48.39 ± 0.22	48.98 ± 0.35	49.84 ± 0.34
	HPCA	43.05 ± 0.36	43.93 ± 0.23	48.68 ± 0.27	46.05 ± 0.24	43.87 ± 0.28
25%	BP	53.36 ± 0.10	59.11 ± 0.21	60.94 ± 0.15	64.57 ± 0.26	67.17 ± 0.16
	HPCA	49.62 ± 0.36	51.30 ± 0.25	56.14 ± 0.29	53.46 ± 0.28	51.29 ± 0.15
100%	BP	51.67 ± 0.10	60.84 ± 0.19	67.01 ± 0.13	78.85 ± 0.10	80.74 ± 0.05
	HPCA	60.94 ± 0.09	62.24 ± 0.15	64.17 ± 0.22	61.27 ± 0.24	59.51 ± 0.20

particular, the improvement becomes significant in correspondence of network layers 3 and 4 in the sample efficiency regimes between 2% and 5%. Note also that layer 3 generally offers absolute highest accuracy for all efficiency regimes, when HPCA is used. In these cases, we observe peaks of improvement over 2 percent points. As before, for efficiency regimes higher than 4% BP starts to provide better accuracy in the higher layers of the network. However, HPCA is still better than BP, with 100% efficiency regime, when tested on Layer 1 and 2. This can be explained by the fact that CIFAR100 offers a more difficult scenario than CIFAR10, and back propagation has more problems than before in backpropagating the error signal to the initial layers of the network. Differently, unsupervised Hebbian learning has most of its effects in the very first layers of the network.

7.3. Tiny ImageNet

Further experiments on Tiny ImageNet allowed us to validate the scalability of our previous observations to larger datasets. Tiny ImageNet has 200 classes and the training set consists of 100,000 samples (90,000 of which are used for training and 10,000 for validation).

Results are reported in Tab. 3, where the top-5 accuracy measures are shown, along with their 95% confidence interval. Again, results confirm our observations. In regimes where a limited number of labeled samples is available (between 1% and 5%), the Hebbian approach outperforms BP, in almost all the cases. When the number of available labeled samples becomes larger, BP is able to exploit supervision and improve over HPCA. Specifically, HPCA outperforms BP in all layers up to 4% sample efficiency regime. In fact, with CIFAR10 and CIFAR100, BP started to outperform HPCA on layer 5 at 4% regimes. Here, with 4% sample efficiency regime, HPCA is still better than BP in all layers. This is probably due to the fact that the number of classes in Tiny ImageNet is higher and using just a few samples does not allow back propagation to correctly adapt the behaviour of network layers. In addition, we can observe that HPCA generally outperforms backprop by roughly 1-2 percent points, reaching a peak of almost 3 percent points on layer 3, in the 4% sample efficiency regime. With higher efficiency regimes, BP begins to outperform HPCA, starting from the higher layers. At 100% sample efficiency regime, BP outperforms HPCA on all layers. This is probably due to the fact that 90,000 labeled training samples are sufficient for BP to cor-

Table 3: TinyImageNet accuracy (top-5) and 95% confidence intervals obtained with a linear classifier on top of various layers, for the various sample efficiency regimes. Results obtained with backprop (BP) and Hebbian PCA (HPCA) training are compared. It is possible to observe that, in regimes where the number of available samples is low (roughly between 1% and 5% of the total available samples), HPCA outperforms backprop in almost all the cases, leading to an improvement up to almost 3% (on layer 3, in the 4% regime).

Regimes	Method	L1	L2	L3	L4	L5
1%	BP	9.89 \pm 0.15	10.10 \pm 0.26	9.99 \pm 0.17	9.15 \pm 0.23	9.53 \pm 0.21
	HPCA	10.83 \pm 0.28	10.87 \pm 0.26	11.85 \pm 0.19	10.84 \pm 0.26	10.86 \pm 0.23
2%	BP	12.76 \pm 0.27	12.84 \pm 0.14	13.95 \pm 0.34	13.04 \pm 0.15	13.48 \pm 0.39
	HPCA	13.84 \pm 0.17	14.35 \pm 0.15	16.18 \pm 0.15	14.52 \pm 0.32	14.03 \pm 0.15
3%	BP	14.12 \pm 0.20	14.65 \pm 0.57	16.50 \pm 0.32	15.76 \pm 0.27	15.99 \pm 0.38
	HPCA	16.13 \pm 0.14	16.32 \pm 0.33	18.87 \pm 0.29	17.04 \pm 0.26	16.38 \pm 0.25
4%	BP	15.44 \pm 0.42	16.72 \pm 0.31	18.36 \pm 0.22	17.85 \pm 0.16	17.84 \pm 0.19
	HPCA	17.64 \pm 0.49	18.27 \pm 0.34	21.07 \pm 0.17	19.16 \pm 0.33	18.13 \pm 0.39
5%	BP	16.75 \pm 0.25	17.94 \pm 0.25	20.26 \pm 0.21	20.15 \pm 0.35	19.84 \pm 0.36
	HPCA	18.93 \pm 0.14	19.67 \pm 0.36	22.65 \pm 0.35	21.01 \pm 0.38	19.57 \pm 0.15
10%	BP	20.26 \pm 0.18	23.12 \pm 0.14	27.05 \pm 0.20	27.30 \pm 0.20	27.21 \pm 0.29
	HPCA	22.15 \pm 0.43	23.69 \pm 0.24	27.02 \pm 0.24	25.73 \pm 0.34	23.08 \pm 0.17
25%	BP	28.97 \pm 0.26	32.63 \pm 0.36	37.38 \pm 0.13	38.81 \pm 0.20	38.80 \pm 0.39
	HPCA	27.05 \pm 0.47	28.39 \pm 0.34	32.08 \pm 0.19	31.30 \pm 0.26	29.51 \pm 0.23
100%	BP	42.89 \pm 0.13	49.94 \pm 0.13	54.54 \pm 0.27	57.00 \pm 0.16	57.50 \pm 0.16
	HPCA	35.74 \pm 0.15	38.29 \pm 0.19	38.78 \pm 0.07	38.61 \pm 0.21	36.99 \pm 0.36

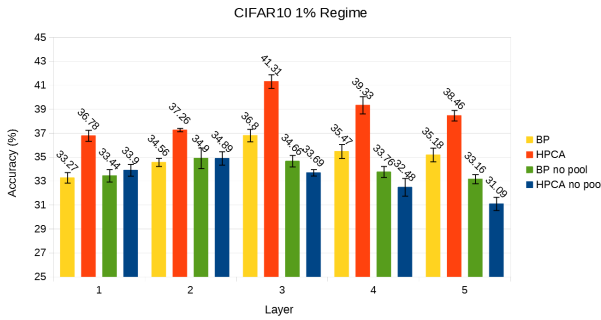
rectly train all network layers, exploiting the supervised information.

7.4. Effect of pooling layers

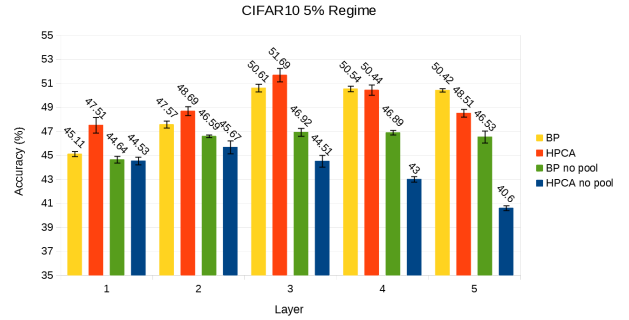
From the results presented so far, it is possible to observe that higher results for low sample efficiency regimes (1-5%) are generally achieved in correspondence of layer 3. We note also that in Layer 1 and 3 of our network, as show in Fig. 1, we have max-pooling operations. We performed further experiments in order to evaluate the impact of pooling layers on the final results. In this subsection, we discuss the results of previous experiments executed in a network where all max-pooling operations were eliminated. In Figs. 6, 7, 8, we show the accuracy obtained for the 1% and 5% sample efficiency regimes, on the CIFAR10, CIFAR100 and Tiny ImageNet datasets. Yellow and red bars correspond to experiments executed with the original network, trained with BP and HPCA, respectively. Green and blue bars corresponds to experiments executed with the network where max-pooling was eliminated, also trained with BP and HPCA respectively. It can be clearly seen the peak of accuracy, occurring at layer 3, for all experiments executed with the original network. Similarly, we can see that the peak disappeared with the experiments executed without max-

pooling. In fact, it seems that the peak moved at layer 2. However, it is within the reported confidence interval of the adjacent layers, so the difference is not statistically significant. In addition, when max-pooling is not used, we report a general decrease of performance. This confirms that max-pooling is a relevant element and its use significantly helps our semi-supervised approach. Note that also in case of BP experiments, without max-pooling, significantly lower results were obtained w.r.t. the highest accuracy, which was achieved with HPCA training in conjunction with pooling layers.

Max-pooling clearly helps the network to produce better feature maps to be used by the linear classifier. In fact, adding consecutive convolutional layers produces neurons with increasingly larger receptive field size. However neurons activations corresponding to adjacent areas, in a given feature map, will be highly correlated. The effect of pooling is to reduce this correlation. This turns out to be very helpful for the final classifiers, which can better handle feature maps of lower dimension and with less redundant information, making it easier to discover relationships between features and target classes.

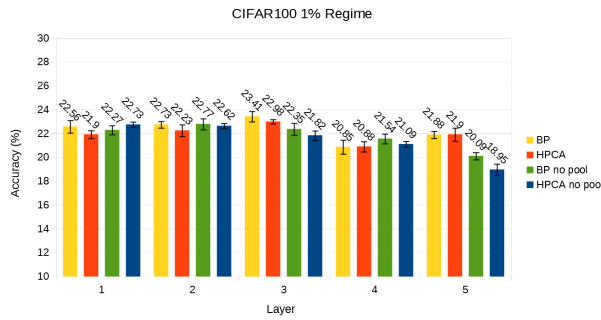


(a) Accuracy results (top-1) in the 1% sample efficiency regime.

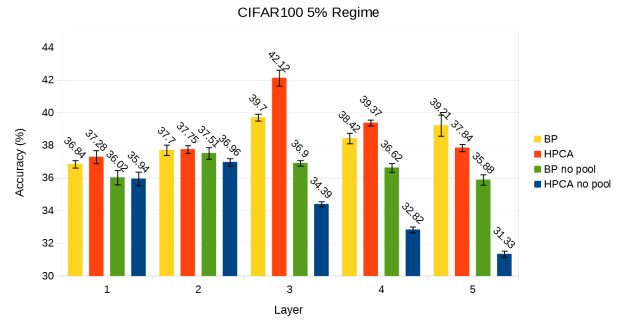


(b) Accuracy results (top-1) in the 5% sample efficiency regime.

Figure 6: Comparison of network architectures with and without pooling on the CIFAR10 dataset.

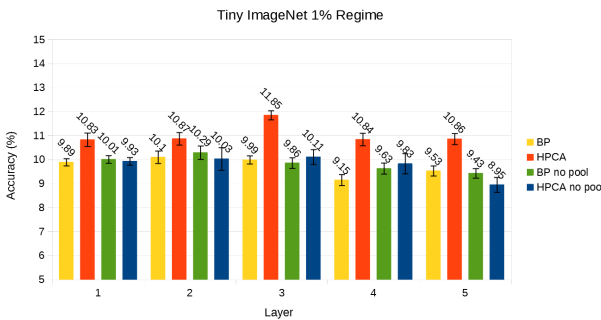


(a) Accuracy results (top-5) in the 1% sample efficiency regime.

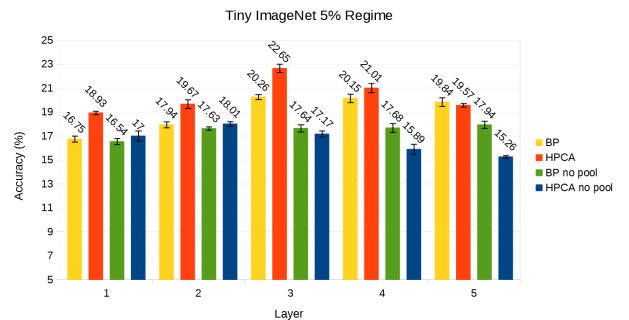


(b) Accuracy results (top-5) in the 5% sample efficiency regime.

Figure 7: Comparison of network architectures with and without pooling on the CIFAR100 dataset.



(a) Accuracy results (top-5) in the 1% sample efficiency regime.



(b) Accuracy results (top-5) in the 5% sample efficiency regime.

Figure 8: Comparison of network architectures with and without pooling on the Tiny ImageNet dataset.

8. Conclusions and future work

In summary, our results suggest that our semi-supervised approach leveraging on Hebbian learning is preferable w.r.t. backprop to perform training in low sample efficiency regimes where only a limited number of labeled samples is available. Our results on CIFAR10, CIFAR100, and Tiny ImageNet show that Hebbian PCA performs better than backprop in sample efficiency regimes in which only a small portion of the training set (between 1% and 5%) is assumed to be labeled. Therefore, our method is preferable in scenarios in which manually labeling a large number of training samples would be too expensive, while gathering unlabeled samples is relatively cheap.

In future work, further improvements might come from exploring more complex feature extraction strategy, which can also be formulated as Hebbian learning variants, such as Kernel-PCA [37] and Independent Component Analysis (ICA) [38]. In addition, it would be interesting to replicate this work also to the context of Spiking Neural Networks (SNNs), where the Hebbian principle is implemented by the Spike Timing Dependent Plasticity (STDP) learning rule [12]. SNNs are more realistic models of biological neural computation, which use pulses (called *spikes*) to encode signals, rather than continuous values. This communication paradigm is the key towards energy-efficient computation in the brain [39], and is being currently implemented in *neuromorphic hardware* [40, 41]. In this scenario, it is necessary to map the variants of the Hebbian rule to corresponding STDP variants and test their effectiveness for SNN training. Finally, an exploration on the behavior of such algorithms w.r.t. adversarial examples also deserves attention.

9. Acknowledgements

This work was partially supported by the H2020 project AI4EU under GA 825619 and by the H2020 project AI4Media under GA 951911.

References

- [1] K. He, X. Zhang, S. Ren, J. Sun, Deep residual learning for image recognition, in: Proceedings of the IEEE conference on computer vision and pattern recognition, 2016, pp. 770–778.
- [2] D. Silver, A. Huang, C. J. Maddison, A. Guez, L. Sifre, G. Van Den Driessche, J. Schrittwieser, I. Antonoglou, V. Panneershelvam, M. Lanctot, et al., Mastering the game of go with deep neural networks and tree search, *nature* 529 (7587) (2016) 484.
- [3] J. Devlin, M.-W. Chang, K. Lee, K. Toutanova, Bert: Pre-training of deep bidirectional transformers for language understanding, arXiv preprint arXiv:1810.04805 (2018).
- [4] Y. Bengio, P. Lamblin, D. Popovici, H. Larochelle, Greedy layer-wise training of deep networks, in: Advances in neural information processing systems, 2007, pp. 153–160.
- [5] H. Larochelle, Y. Bengio, J. Louradour, P. Lamblin, Exploring strategies for training deep neural networks., *Journal of machine learning research* 10 (1) (2009).
- [6] J. Weston, F. Ratle, H. Mobahi, R. Collobert, Deep learning via semi-supervised embedding, in: *Neural networks: Tricks of the trade*, Springer, 2012, pp. 639–655.
- [7] D. P. Kingma, S. Mohamed, D. Jimenez Rezende, M. Welling, Semi-supervised learning with deep generative models, *Advances in neural information processing systems* 27 (2014) 3581–3589.
- [8] A. Rasmus, M. Berglund, M. Honkala, H. Valpola, T. Raiko, Semi-supervised learning with ladder networks, in: *Advances in neural information processing systems*, 2015, pp. 3546–3554.
- [9] Y. Zhang, K. Lee, H. Lee, Augmenting supervised neural networks with unsupervised objectives for large-scale image classification, in: *International conference on machine learning*, 2016, pp. 612–621.
- [10] T. Chen, S. Kornblith, M. Norouzi, G. Hinton, A simple framework for contrastive learning of visual representations, in: *International conference on machine learning*, PMLR, 2020, pp. 1597–1607.
- [11] S. Haykin, *Neural networks and learning machines*, 3rd Edition, Pearson, 2009.
- [12] W. Gerstner, W. M. Kistler, *Spiking neuron models: Single neurons, populations, plasticity*, Cambridge university press, 2002.
- [13] R. C. O’Reilly, Y. Munakata, *Computational explorations in cognitive neuroscience: Understanding the mind by simulating the brain*, MIT press, 2000.
- [14] J. Weston, S. Chopra, A. Bordes, Memory networks, arXiv preprint arXiv:1410.3916 (2014).
- [15] S. Grossberg, Adaptive pattern classification and universal recoding: I. parallel development and coding of neural feature detectors, *Biological cybernetics* 23 (3) (1976) 121–134.
- [16] T. Kohonen, Self-organized formation of topologically correct feature maps, *Biological cybernetics* 43 (1) (1982) 59–69.
- [17] T. D. Sanger, Optimal unsupervised learning in a single-layer linear feedforward neural network, *Neural networks* 2 (6) (1989) 459–473.
- [18] J. Karhunen, J. Joutsensalo, Generalizations of principal component analysis, optimization problems, and neural networks, *Neural Networks* 8 (4) (1995) 549–562.
- [19] S. Becker, M. Plumbley, Unsupervised neural network learning procedures for feature extraction and classification, *Applied Intelligence* 6 (3) (1996) 185–203.
- [20] C. Pehlevan, T. Hu, D. B. Chklovskii, A hebbian/anti-hebbian neural network for linear subspace learning: A derivation from multidimensional scaling of streaming data, *Neural computation* 27 (7) (2015) 1461–1495.
- [21] C. Pehlevan, D. B. Chklovskii, Optimization theory of hebbian/anti-hebbian networks for pca and whitening, in: *2015 53rd Annual Allerton Conference on Communication, Control, and Computing (Allerton)*, IEEE, 2015, pp. 1458–1465.
- [22] A. Wadhwa, U. Madhoo, Learning sparse, distributed representations using the hebbian principle, arXiv preprint arXiv:1611.04228 (2016).
- [23] A. Wadhwa, U. Madhoo, Bottom-up deep learning using the hebbian principle (2016).
- [24] Y. Bahroun, A. Soltoggio, Online representation learning with single and multi-layer hebbian networks for image classification, in: *International Conference on Artificial Neural Networks*, Springer, 2017, pp. 354–363.
- [25] D. Krotov, J. J. Hopfield, Unsupervised learning by competing

- hidden units, *Proceedings of the National Academy of Sciences* 116 (16) (2019) 7723–7731.
- [26] G. Amato, F. Carrara, F. Falchi, C. Gennaro, G. Lagani, Hebbian learning meets deep convolutional neural networks, in: *International Conference on Image Analysis and Processing*, Springer, 2019, pp. 324–334.
- [27] G. Lagani, Hebbian learning algorithms for training convolutional neural networks, Master’s thesis, School of Engineering, University of Pisa, Italy (2019).
URL <https://etd.adm.unipi.it/theses/available/etd-03292019-220853/>
- [28] A. Magotra, J. kim, Transfer learning for image classification using hebbian plasticity principles, in: *Proceedings of the 2019 3rd International Conference on Computer Science and Artificial Intelligence*, 2019, pp. 233–238.
- [29] A. Magotra, J. Kim, Improvement of heterogeneous transfer learning efficiency by using hebbian learning principle, *Applied Sciences* 10 (16) (2020) 5631.
- [30] F. J. A. Canto, Convolutional neural networks with hebbian-based rules in online transfer learning, in: *Mexican International Conference on Artificial Intelligence*, Springer, 2020, pp. 35–49.
- [31] J. Yosinski, J. Clune, Y. Bengio, H. Lipson, How transferable are features in deep neural networks?, *arXiv preprint arXiv:1411.1792* (2014).
- [32] P. Földiák, Forming sparse representations by local anti-hebbian learning, *Biological cybernetics* 64 (2) (1990) 165–170.
- [33] B. A. Olshausen, D. J. Field, Emergence of simple-cell receptive field properties by learning a sparse code for natural images, *Nature* 381 (6583) (1996) 607.
- [34] A. Krizhevsky, G. Hinton, Learning multiple layers of features from tiny images (2009).
- [35] J. Wu, Q. Zhang, G. Xu, Tiny imagenet challenge, Tech. rep., Technical report, Stanford University, 2017. Available online at [http ...](http://...) (2017).
- [36] A. Krizhevsky, I. Sutskever, G. E. Hinton, Imagenet classification with deep convolutional neural networks, *Advances in neural information processing systems* (2012).
- [37] B. Schölkopf, A. Smola, K.-R. Müller, Nonlinear component analysis as a kernel eigenvalue problem, *Neural computation* 10 (5) (1998) 1299–1319.
- [38] A. Hyvarinen, J. Karhunen, E. Oja, Independent component analysis, *Studies in informatics and control* 11 (2) (2002) 205–207.
- [39] F. Javed, Q. He, L. E. Davidson, J. C. Thornton, J. Albu, L. Boxt, N. Krasnow, M. Elia, P. Kang, S. Heshka, et al., Brain and high metabolic rate organ mass: contributions to resting energy expenditure beyond fat-free mass, *The American journal of clinical nutrition* 91 (4) (2010) 907–912.
- [40] S. B. Furber, F. Galluppi, S. Temple, L. A. Plana, The spinnaker project, *Proceedings of the IEEE* 102 (5) (2014) 652–665.
- [41] X. Wu, V. Saxena, K. Zhu, S. Balagopal, A cmos spiking neuron for brain-inspired neural networks with resistive synapses and in situ learning, *IEEE Transactions on Circuits and Systems II: Express Briefs* 62 (11) (2015) 1088–1092.